BMC Cancer

RESEARCH

Open Access

The Hippo pathway terminal effector TAZ/WWTR1 mediates oxaliplatin sensitivity in p53 proficient colon cancer cells

Věra Slaninová[1†], Lisa Heron-Milhavet[1†], Mathilde Robin[1,2,3], Laura Jeanson[1], Adam Aissanou[1], Diala Kantar[1], Diego Tosi[1,3], Laurent Bréhélin[2], Céline Gongora[4*] and Alexandre Djiane[1,4*]

Abstract

YAP and TAZ, the Hippo pathway terminal transcriptional activators, are frequently upregulated in cancers. In tumor cells, they have been mainly associated with increased tumorigenesis controlling different aspects from cell cycle regulation, stemness, or resistance to chemotherapies. In fewer cases, they have also been shown to oppose cancer progression, including by promoting cell death through the action of the p73/YAP transcriptional complex, in particular after chemotherapeutic drug exposure. Using HCT116 cells, we show here that oxaliplatin treatment led to core Hippo pathway down-regulation and nuclear accumulation of TAZ. We further show that TAZ was required for the increased sensitivity of HCT116 cells to oxaliplatin, an effect that appeared independent of p73, but which required the nuclear relocalization of TAZ. Accordingly, Verteporfin and CA3, two drugs affecting the activity of YAP and TAZ, showed antagonistic effects with oxaliplatin in co-treatments. Importantly, using several colorectal cell lines, we show that the sensitizing action of TAZ to oxaliplatin is dependent on the p53 status of the cells. Our results support thus an early action of TAZ to sensitize cells to oxaliplatin, consistent with a model in which nuclear TAZ in the context of DNA damage and p53 activity pushes cells towards apoptosis.

Keywords Oxaliplatin, Colon cancer, Hippo signaling, TAZ, p53

Introduction

Colorectal cancer (CRC) is the third leading cause of cancer-related death worldwide [43]. Thirty percent of patients present synchronous metastases and 50–60% will develop metastases that will require chemotherapy. The current management of advanced or metastatic CRC is based on fluoropyrimidine (5-FU), oxaliplatin and irinotecan as single agents or more often in combination (e.g. FOLFOX, FOLFIRI, or FOLFIRINOX; [63]). Chemotherapy is combined with targeted therapy including monoclonal antibodies against EGFR (e.g. cetuximab and panitumumab) or VEGF (bevacizumab), tyrosine kinase inhibitors (e.g. regorafenib), and immune checkpoint blockade agents for patients with MSI-High tumors (e.g. pembrolizumab; [63]).

Oxaliplatin is a third-generation platinum antitumor compound with a 1,2-diaminocyclohexane (DACH) ligand [9, 44]. It induces mainly intra-strand crosslinks, but also inter-strand crosslinks and DNA–protein crosslinks that stop DNA replication and transcription, leading to apoptotic cell death [40, 61, 62]. Oxaliplatin

†Věra Slaninová and Lisa Heron-Milhavet contributed equally to this work.

*Correspondence:
Céline Gongora
celine.gongora@inserm.fr
Alexandre Djiane
alexandre.djiane@inserm.fr
[1] IRCM, Univ Montpellier, Inserm, ICM, Montpellier, France
[2] LIRMM, Univ Montpellier, Inserm, CNRS, Montpellier, France
[3] Fondazione Gianni Bonadonna, Milan, Italy
[4] IRCM, Univ Montpellier, Inserm, ICM, CNRS, Montpellier, France

exerts its anti-tumor effect also by inducing immunogenic cell death [55]. Resistance to oxaliplatin can be either intrinsic (primary resistance) or acquired (secondary resistance), and is usually tackled by combining drugs to expose tumoral cells weaknesses or inhibit alternative survival pathways [59]. Despite intense research efforts in this field, more information on the molecular mechanisms underlying oxaliplatin mechanism of action are needed to develop new treatment strategies and improve the therapeutic response rate.

The Hippo signaling pathway represents an evolutionarily highly conserved growth control pathway. First discovered through genetic screens in *Drosophila*, it consists of a central cascade of core kinases: MST1/2 and LATS1/2 (homologues of *Drosophila* Hippo and Warts; [17, 41, 66]). When activated, LATS1/2 phosphorylate YAP and WWTR1/TAZ (homologues of *Drosophila* Yki), two partly redundant transcriptional co-activators which represent the terminal effectors of the Hippo pathway [45]. Phosphorylated YAP and TAZ are retained in the cytoplasm through binding to 14-3-3 proteins and sent for proteasomal degradation. When the Hippo pathway is not activated, hypo-phosphorylated YAP/TAZ enter the nucleus and bind to specific transcription factors (TFs) to turn on the transcription of target genes. The best characterized TF partners for YAP and TAZ are the TEADs (TEAD1-4, homologues of *Drosophila* Scalloped; [17, 41, 66]). While depending on cell type, the classic target genes include genes involved in proliferation, resistance to apoptosis, cytoskeletal remodeling, or stemness [46, 54, 57]. But YAP/TAZ nucleo-cytoplasmic localization (and activity) is also controlled by mechanical cues relayed by the actin cytoskeleton, or by cytoplasmic trapping proteins such as AMOTs [17, 41, 66]. Importantly, the nuclear retention of YAP and TAZ is favored by tyrosine phosphorylation by different kinases, and in particular SRC and YES [8, 13, 30].

The Hippo pathway has been primarily described as a tumor suppressive pathway in a wide variety of solid tumors [22, 29, 38, 56, 66] preventing the pro-tumoral effect of YAP/TAZ. However, in CRCs the role of the Hippo pathway and of YAP and TAZ appears more complex. Several studies point towards a classic pro-tumoral role for YAP and TAZ. In CRC patients tumor samples, high expression and nuclear localization of YAP correlated strongly with disease evolution and bad prognosis [33, 51], or with resistance to treatments such as 5FU or cetuximab [22, 27, 58]. Furthermore, invalidating YAP could blunt tumorigenic behaviors both in mice CRC models [48] or in the metastatic HCT116 CRC cell line [23]. However, YAP could exhibit a tumor suppressive role in CRCs. Studies in genetic mouse models have shown that YAP/TAZ restricts canonical Wnt/β-Catenin signaling thus preventing intestinal stem cells amplification, and could act as tumor suppressors in CRCs [3–5]. Similarly, the loss of core Hippo kinases (LATS/MST) was recently shown to inhibit tumor progression in Apc mutant mouse models and in patients-derived xenografts models [11, 31].

The tumor suppressive role of YAP in CRC is further supported by its reported role in response to DNA damage inducer drugs. Studies have shown that, in different cell lines including CRC lines, cell death in response to cisplatin, doxorubicin, or etoposide, is mediated by p73, a protein related to the tumor-suppressor p53. Following treatments, a YAP/p73 complex accumulates in the nucleus, and triggers the transcription of p73 target genes involved in cell death [26, 52, 53]. The direct interaction between YAP and p73 is proposed to prevent p73 destabilization by the E3-Ubiquitin Ligase ITCH [28, 52]. This pro-apoptotic role of YAP is reminiscent to a similar role of Yki in *Drosophila* (a Yki/p53 complex; [12]). Importantly, this appears specific to YAP, since TAZ cannot bind to p73, further suggesting that YAP and TAZ, while performing redundant roles, also possess specific activities [45].

Given that oxaliplatin constitute one of the most used drugs in the treatment of CRCs, it is important to evaluate its effects with respect to the Hippo pathway and to YAP/TAZ which can elicit conflicting roles to oppose or promote CRC tumorigenesis. We show here that upon treatment with oxaliplatin, TAZ accumulated in the nucleus of p53 wild-type CRC cell lines. We further show that TAZ was required for early sensitivity of HCT116 to oxaliplatin. Interestingly, the nuclear localization of TAZ was important, and drugs preventing this such as Dasatinib antagonized the effect of oxaliplatin. These results support an early anti-tumoral role of YAP and TAZ in response to oxaliplatin suggesting particular attention to sequence of treatments and drug combinations should be paid when considering potential future drugging of YAP/TAZ signaling in the treatment of CRCs, in particular for tumors with wild-type p53.

Materials and methods

shRNA construction

shRNA directed against human *YAP*, or the non-relevant *Luciferase* gene were designed by adding to the selected targeted sequences, overhangs corresponding to BamHI and EcoRI cloning sites at the 5'end of forward and reverse strand, respectively. Resulting oligos were then annealed together and cloned into the pSIREN-RetroQ vector (TaKaRa) according to the manufacturer's protocol between BamHI and EcoRI cloning sites.

Targeted sequences:

shRNA-YAP(3619): CAATCACTGTGTTGTATAT
shRNA-Luciferase: CGTACGCGGAATACTTCGA

Cell culture and cell transfections

Certified Human HCT116 and LoVo colorectal cancer cell lines (RRID:CVCL_0291, RRID:CVCL_0399) were obtained from LGC Standards (ATCC-CCL-247, ATCC-CCL-229). Caco-2, HT-29, and SW480 cells were obtained from ATCC (RRID:CVCL_0025, ATCC-HTB-37; RRID:CVCL_0320, ATCC-HTB-38; RRID:CVCL_0546, ATCC-CCL-228). Human HCT 116 p53 mutant cells were from [7]. Cells were cultured in RPMI1640 supplemented with 10% FBS at 37 °C in a humidified atmosphere with 5% CO_2. All experiments were performed with mycoplasma-free cells. No antibiotics were used to avoid any cross-reaction with the Oxaliplatin treatment.

Mutational status of the cell lines used

	p53 status	APC status	CTNNB1status
HCT116	wild-type	wild-type	mutated
HCT116 p53 mut	exon 1 deletion	wild-type	mutated
LoVo	wild-type	mutated	wild-type
Caco-2	E204*	mutated	mutated
HT-29	R273H	mutated	wild-type
SW480	R273H, P309S	mutated	wild-type

HCT116 cells expressing shRNA against *YAP*, or *Luciferase* (Luc; control) were obtained by retroviral gene transduction of the corresponding pSIREN vectors. Retroviral particles were produced in HEK293 cells and subsequently used to infect HCT116 cells. Positive clones were selected with 1 µg/mL puromycin and pooled together.

HCT116-*shYAP/siTAZ* cells were created by transfecting 100 nM of *TAZ siRNA* (Dharmacon siGENOME SMARTpool #M-016083-00-0005) into HCT116-*shYAP* cells using Lipofectamine 2000 (Invitrogen) according to manufacturer's protocol. As a negative control, 100 nM of *siScrambled* (D-001206-13) was transfected into HCT116-*shLuc* cells.

All human cell lines have been authenticated using STR profiling within the last three years.

Murine Taz was expressed by transfecting cells with pEF-TAZ-N-Flag from Michael Yaffe (Addgene #19025; RRID:Addgene_19025; [19]).

Apart from IC50 calculations, or 2D treatments matrices, cells were analyzed after 24 h of treatment with oxaliplatin. For this short treatment there was no significant change in cellular density and analyses were performed at circa 70% confluency.

RNA-Seq

HCT116 cells were plated to reach 60 to 70% of confluence and treated with 0.5 µM Oxaliplatin (IC_{50}) for 24 h. RNA was extracted using RNeasy plus mini kit (Qiagen), quantified, and analyzed for its integrity number (RIN) using a Bioanalyzer (Agilent 2100 at the IRMB: https://irmb-montpellier.fr/single-service/transcriptome-ngs/). RNA (1 µg) with RIN between 8 and 10 were sent for RNA-Sequencing analysis to Fasteris biotechnology company (http://www.fasteris.com). After library preparation, sequencing was performed on the Illumina NovaSeq 6000 platform (S1 2x100 full FC). Mapping on the human genome GRCh38 was performed using the protocol STAR 2.7.5b leading to 80–100 Millions reads per condition. Normalization and pairwise differential expression analyses were performed using the R package DESeq2 (2.13) [2].

Western blotting

Proteins from transfected untreated and treated HCT116 cells were extracted, analyzed by SDS-PAGE. Dilutions and antibodies' references are listed below (Cell Signaling Technology: CST).

Antibody	Dilution	Reference
Flag M2	1/2000	Sigma-Aldrich #F1804
GAPDH	1/3000	Proteintech #60004
Histone H3	1/1000	CST #4499
LATS1	1/1000	CST #3477
MOB1	1/1000	CST #13730
p-MOB1	1/1000	CST #8699
MST1	1/1000	CST #3682
p-MST1/2	1/1000	CST #49332
NF2	1/1000	Proteintech #26686-1-AP
p53	1/5000	Proteintech #10442-1-AP
p63	1/250	Santa Cruz #sc25268
p73	1/1000	CST #14620
p-SRC Y416	1/1000	CST #2105
TAZ	1/1000	CST #4883
TEAD4	1/250	Santa Cruz #sc101184
Tubulin	1/10000	Sigma-Aldrich #T6074
YAP	1/1000	CST #14074
p-YAP S127	1/1000	CST #13008

Immunoprecipitation and co-immunoprecipitation

Protein extracts were prepared in lysis buffer (NaCl 150 mM, Tris pH 7.4 10 mM, EDTA 1 mM, Triton X-100 1%, NP-40 0.5%, cOmplete, EDTA-free protease inhibitors (Roche #11873580001) for 30 min on ice before centrifugation. Immunoprecipitations were performed overnight at 4 °C on a rocking wheel using

mouse EZview Red anti-Flag M2 affinity gel (Sigma-Aldrich #F1804) after transfections of either p2xFlag CMV2 (empty vector), p2xFlag CMV2-YAP2 (YAP1; Addgene #19045) or p2xFlag CMV2-WWTR1 (TAZ). After Flag immunoprecipitation, washes in lysis buffer were performed, followed by protein elution by competition with 3XFLAG peptide (150 ng/µL final concentration) during 1 h at 4 °C. The different immunoprecipitates were then subjected to Western blotting for detection of protein complexes.

Immunofluorescence

Cells seeded on glass coverslips were fixed 10 min in paraformaldehyde (4%), before being permeabilized in PBS / 0.1% TritonX-100 for 10 min. After blocking in PBS / 0.5% BSA, cells were incubated with primary antibodies overnight at 4C. Primary antibodies used are listed below. Secondary Alexa Fluor Antibodies (1/600; Invitrogen) were used as described previously [20] for 1 h at room temperature before mounting the coverslips with Vectashield (Vector Laboratories #H-1200) and imaging on Zeiss Apotome or Leica Thunder microscopes.

Antibodies used were rabbit anti-53BP1 (1/100; CST #4937), mouse anti-phospho-Histone H2AX clone JBW301 (1/200; Millipore #05–636), anti-TAZ (1/100; CST #4883), mouse anti-TEAD4 (1/50; Santa Cruz #sc101184), and rabbit anti-YAP (1/100; CST #14074).

Nuclear staining quantifications in HCT116 cells

Quantification was performed using ImageJ. Binary mask corresponding to the cell nuclei was based on DAPI staining. Two nuclei touching each other (and therefore recognized as one on binary mask) were manually separated by drawing a 2-pixel line between them. All incomplete nuclei on the edge of the image as well as those that were in mitosis or mechanically damaged were excluded from the analysis. The total signal was calculated as "corrected total cell fluorescence" (CTCF) according to the following formula:

$$CTCF = Integrated\ Density - (Area\ of\ selected\ cell * Mean\ fluorescence\ of\ the\ background)$$

Background fluorescence was measured on three different spots (roughly the size of cell nucleus) outside of the cell. In case of 53BP1 and γH2AX staining, the whole area covered by the nuclear mask was quantified as one. For YAP and TAZ nuclear staining, each cell was quantified separately using particle analysis tool. Cytoplasmic levels of YAP and TAZ were not quantified due to the small size of the cytoplasm in HCT116 cells.

IC50 calculation and cytotoxicity

Cell growth inhibition and cell viability after incubation with Oxaliplatin (Sigma Aldrich #O9512), Verteporfin (Sigma Aldrich #SML0534), CA3 (CIL56, Selleckchem, #S8661) or Dasatinib (Selleckchem #S1021) were assessed using the sulforhodamine B (SRB) assay. Exponentially growing cells (750 cells/well) were seeded in 96-well plates in RPMI-1640 medium supplemented with 10% FCS. After 24 h, serial dilutions of the tested drugs were added, and each concentration was tested in triplicate. After 96 h, cells were fixed with 10% trichloroacetic acid and stained with 0.4% SRB in 1% acetic acid. SRB-fixed cells were dissolved in 10 mmol/L Tris–HCl and absorbance at 540 nm was read using an MRX plate reader (Dynex, Inc., Vienna, VA, USA). IC50 was determined graphically from the cytotoxicity curves.

For HCT116-*shYAP/siTAZ*, cells were transfected in 6 well plates 24 h before starting the cell growth and cytotoxicity assays.

Quantification of the interaction effect

The interaction between the drugs tested in vitro was investigated with a concentration matrix test, in which increasing concentration of each single drug were assessed with all possible combinations of the other drugs. For each combination, the percentage of expected growing cells in the case of effect independence was calculated according to the Bliss equation [15]:

$$fu_c = fu_A fu_B$$

where fu_c is the expected fraction of cells unaffected by the drug combination in the case of effect independence, and fu_A and fu_B are the fractions of cells unaffected by treatment *A* and *B,* respectively. The difference between the fu_c value and the fraction of living cells in the cytotoxicity test was considered as an estimation of the interaction effect, with positive values indicating synergism and negative values antagonism.

Results and discussion

Oxaliplatin treatment triggers an early cell death program

Oxaliplatin is a third generation platinum compound widely used as part of the first line of treatment for colon cancer patients in the FOLFOX regimen [9, 44, 63]. Inside cells, oxaliplatin binds DNA, generating adducts which ultimately lead to DNA breaks and replicative stress in proliferating cells. When used on proliferating

cancer cells, oxaliplatin treatment resulted in concentration-dependent cell death. We measured the IC50 of oxaliplatin on HCT116 colon cancer cells at 0.5 µM (Supplemental Figure S1A). This dose reduced the amount of cells by 50% after 4 days of treatment. This dose was about 10 fold lower than the oxaliplatin concentration reported in the blood of treated patients (between 3.7 and 7 µM; [14]). The oxaliplatin dose used in this study was thus compatible with the dose that could be ultimately found at the level of tumors in a clinical setting, and did not represent an acute high concentration treatment, highlighting its relevance for studying cellular responses to oxaliplatin.

When treated with oxaliplatin at IC50, HCT116 cells exhibited clear signs of DNA damage such as accumulation of γH2AX, and 53BP1 puncta in the nuclei (Fig. 1A&B). Consistently, p53, which has been shown to control a specific cell death program in response to severe DNA damage (for recent reviews [1, 39], accumulated strongly 24 h after treatment (Fig. 1C). Intriguingly, the p53 related protein p73, previously reported to accumulate and to mediate cell death in response to DNA-damage inducing drugs such as cisplatin, doxorubicin or etoposide, including in HCT116 cells [26, 52], was destabilized upon oxaliplatin treatment. p63, the third member of the p53 protein family, was not expressed in HCT116, even upon treatment (Fig. 1C).

Oxaliplatin treatment triggers YAP and TAZ nuclear accumulation

Having established a regimen for treating HCT116 cells with oxaliplatin, given the complex reported roles of YAP/TAZ in CRCs (see "Introduction" section), we investigated whether YAP/TAZ could be affected, and thus monitored TEAD, YAP, and TAZ expressions and localizations following oxaliplatin treatment.

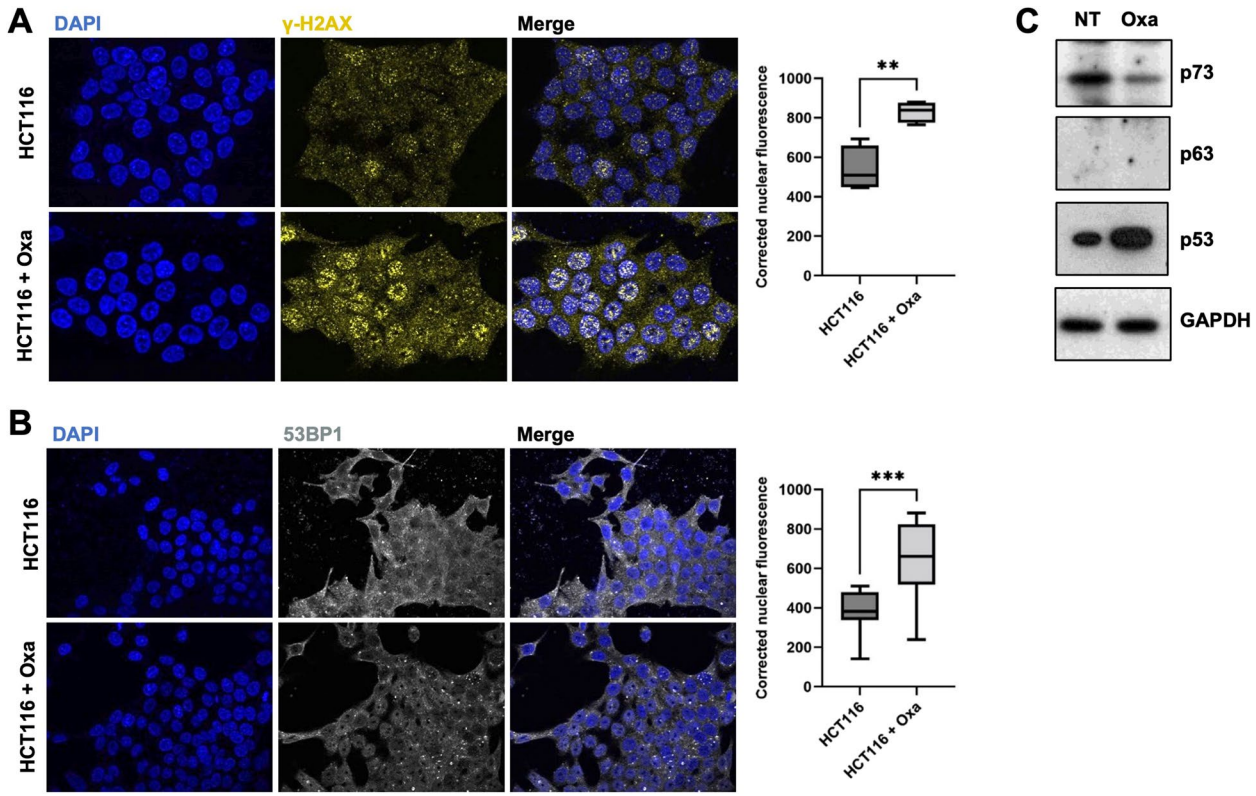

Fig. 1 Oxaliplatin treatment induces DNA damage. **A** Immunofluorescence experiments performed on HCT116 cells treated, or not, with oxaliplatin (0.5 µM) monitoring γ-H2AX (yellow). DAPI (blue) was used to stain DNA and the nuclei. Quantification of the staining is shown on the right side and is represented as the corrected nuclear fluorescence. Data are represented as the mean ± SEM. ($n = 3$). Unpaired two-tailed Student's t-test; ** $p < 0.01$. **B** Immunofluorescence experiments performed on HCT116 cells treated, or not, with oxaliplatin (0.5 µM) monitoring 53BP1 (grey). DAPI (blue) was used to stain DNA and the nuclei. Quantification of the staining is shown on the right side and is represented as the corrected nuclear fluorescence. Data are represented as the mean ± SEM. ($n = 3$). Unpaired two-tailed Student's t-test; *** $p < 0.001$. **C** Western blot analysis showing protein expression of p53 family of proteins in HCT116 treated (Oxa), or not (NT) with oxaliplatin (0.5 µM). GAPDH was used as a loading control ($n = 3$)

After 24 h (or 48 h) of oxaliplatin treatment at the IC50, we did not observe any change in the total levels or in the nuclear localization of TEAD4, the main TEAD paralogue in colon cells (Fig. 2A). However, TAZ and YAP nuclear localizations increased following oxaliplatin treatment in our culture conditions: the TAZ and YAP nuclear staining increased by 60% and 55% respectively when compared to untreated cells (Fig. 2A). TAZ nuclear accumulation was further confirmed by fractionation experiments (Fig. 2C; see "Materials and methods" section). This increase in TAZ nuclear localization was reflected by an increase in total TAZ levels by western blot analysis (Fig. 2B). However, YAP total levels, and more importantly the levels of YAP phosphorylation on Serine 127 (S127) were unchanged (Fig. 2B).

The YAP S127 phosphorylation is deposited by the LATS1/2 Hippo pathway terminal kinases and mediates the cytoplasmic retention of YAP by the 14-3-3 proteins and later targeting for proteasomal degradation [17, 41, 66]. Western-blot analyses on total protein extracts showed that protein levels of several key proteins in the core Hippo pathway were lower after treatments. This was observed both for total proteins (MST1/2, MOB1A, and LATS1) and their activated phosphorylated forms (p-MST1/2, p-MOB1; Fig. 2B). Based on these western-blot analyses, the activity ratio (phosphorylated / total protein) of MOB1A increased slightly during treatment (x1.73) while the activity ratio of MST1 decreased slightly (x0.45). It should be noted here that these activity ratios are based on western-blot after 24 h of treatment and might not reflect the immediate activity of the pathway. Moreover, these activity ratios reflect the normalized activity per unit of protein, but do not reflect the overall integral activity of the pathway. Given that core Hippo pathway proteins were specifically down-regulated after 24 h of treatment (as compared to other proteins which levels remained constant after treatments: GAPDH, TEAD4, NF2, YAP), and that the specific activity of the core kinase MST was slightly reduced, we favor a model where global Hippo pathway activity is lower in response to oxaliplatin, consistent with the increased TAZ levels and increased nuclear TAZ localization (Fig. 2A&C). However, given that levels of phospho-YAP and total YAP remained unchanged, how the Hippo pathway down-regulation could have differing effects on YAP and TAZ remains to be explored. YAP and TAZ appear only partly redundant, and YAP and TAZ specific regulations have been reported [45]. It is noteworthy that an additional phospho-degron is present in TAZ, making it more sensitive to degradation than YAP. This increased sensitivity might magnify TAZ level changes when the Hippo pathway is inhibited by oxaliplatin [4]. The decreased protein levels of different Hippo pathway components in response to oxaliplatin were unlikely due to reduced mRNA abundance, since we did not observe any change when profiling mRNA by RNA-Seq after 24 h of treatment (see paragraph below; Supplemental Table S1), suggesting that it might be a consequence of reduced translation and/or increased protein degradation. Indeed, previous studies have shown that core Hippo pathway components such as LATS1 or MOB1 can be regulated by ubiquitination [18, 32, 47]. Whether oxaliplatin treatment triggers a specific ubiquitin-mediated destabilization of the core Hippo pathway remains however to be studied.

Oxaliplatin does not activate an early Hippo transcriptional programme

Since TAZ accumulated and localized in the nucleus of oxaliplatin-treated cells, we thus wondered whether HCT116 cells treated with oxaliplatin showed a Hippo pathway transcriptional signature. To better understand the cellular responses to oxaliplatin we thus profiled the changes in gene expression after 24 h of exposure at IC 50. This analysis revealed that the expressions of only a limited number of genes were affected (fold change > 1.5, adjusted p-value < 0.05): 253 up-regulated and 111 down-regulated (Supplemental Figure S2 and Supplemental Table 1). Gene ontology enrichment approaches using the g:profiler online tool (Supplemental Table 2; [42])

(See figure on next page.)

Fig. 2 Oxaliplatin treatment triggers YAP and TAZ nuclear accumulation. **A** Immunofluorescence experiments performed on HCT116 cells treated, or not, with oxaliplatin (0.5 µM) monitoring TEAD4 (top panels), YAP (middle panels), and TAZ (bottom panels) nuclear localization (red). DAPI (blue) was used to stain DNA and the nuclei. Quantification of YAP and TAZ stainings are shown on the right side of the figures and are represented as the corrected nuclear fluorescence. Data are represented as the mean ± SEM ($n = 3$). Unpaired two-tailed Student's t-test; **** $p < 0.0001$. **B** Western blot analysis showing protein expression and/or activation of Hippo pathway components in HCT116 cells treated (Oxa), or not (NT) with oxaliplatin (0.5 µM). GAPDH was used as a loading control ($n = 3$). **B'** Quantification of the ratio Oxa/NT of the western-blots shown in B after normalization by GAPDH intensity. Average is shown with standard deviation. Unpaired two-tailed t-test; ** $p < 0.01$, *** $p < 0.001$, ns non-significant. **C** Western blot analysis after subcellular fractionation showing the relative amount of YAP and TAZ protein in the nuclear fraction of HCT116 cells treated (Oxa), or not (NT) with oxaliplatin (0.5 µM). Histone H3 was used as a nuclear loading control for the fractionation ($n = 3$). **C'** Quantification of the ratio Oxa/NT of the western-blots shown in B after normalization by Histone H3 intensity. Average is shown with standard deviation. Unpaired two-tailed t-test; ** $p < 0.01$, *** $p < 0.001$, ns non-significant

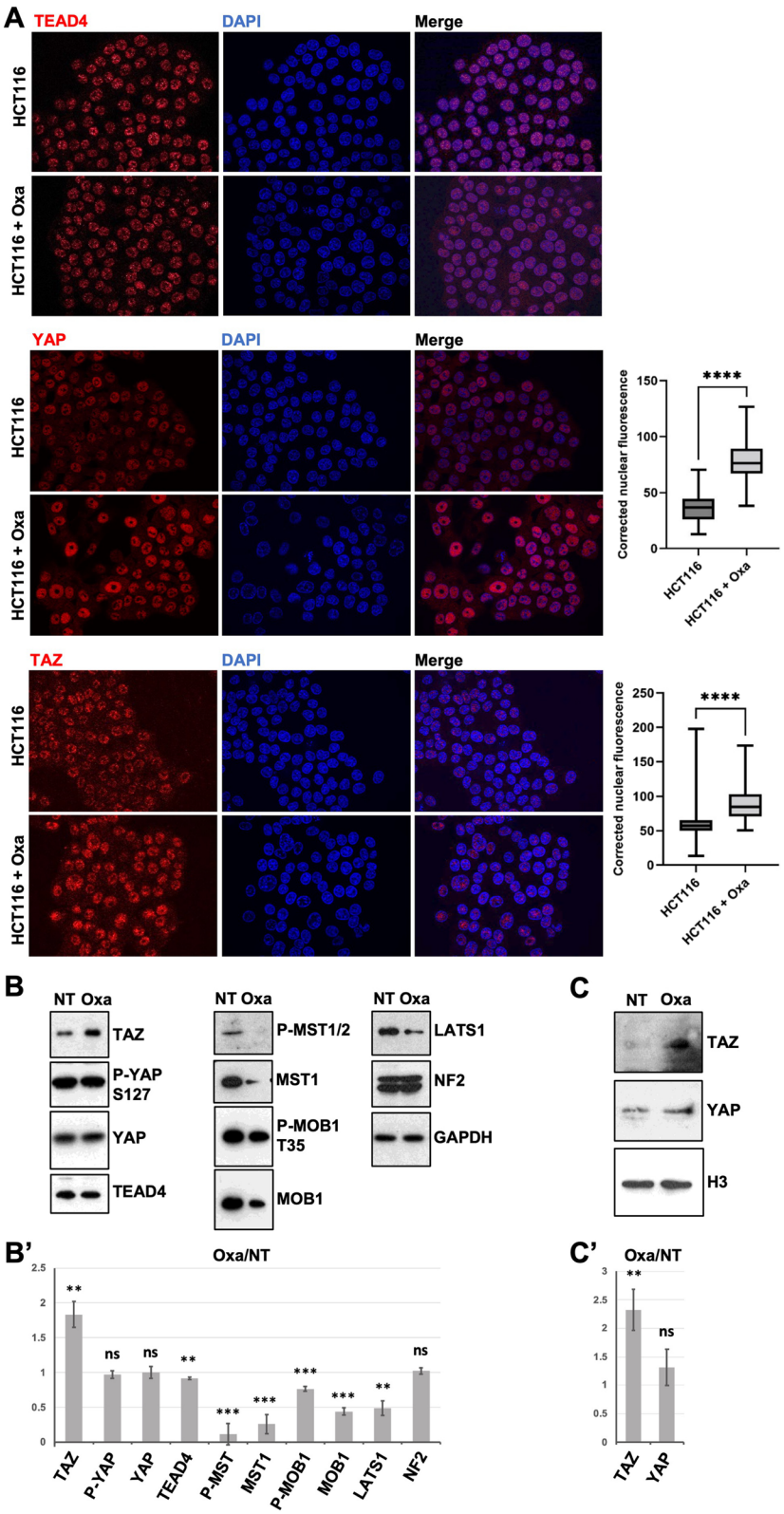

Fig. 2 (See legend on previous page.)

highlighted that amongst the main cellular processes controlled by the upregulated genes were DNA damage response (GO:0044819 mitotic G1/S transition checkpoint signaling; GO:0000077 DNA damage checkpoint signaling…), apoptosis and cell death (GO:0045569 TRAIL binding; GO:0008219 cell death; GO:0012501 programmed cell death; GO:0006915 apoptotic process …), and p53 response (GO:0072331 signal transduction by p53 class mediator), consistent with the known role of oxaliplatin generating adducts on the DNA. Indeed, many genes up-regulated have previously been associated with p53 signaling, and represent p53 canonical target genes such as CDKN1A/P21, P53I3, BAX, or TIGAR (REAC:R-HSA-3700989 Transcriptional Regulation by p53; WP:WP4963 p53 transcriptional gene network). While up-regulated genes controlled mainly cell death programs, the down-regulated genes were involved in DNA replication (GO:0006260) and cell cycle (GO:0007049) consistent with the well documented effect of DNA damage on blocking cell cycle and proliferation [1].

Amongst the genes mis-regulated were also genes related to inflammation and immune cell recruitment (e.g. the upregulated genes CXCR2, EBI3/IL-27, or NLRP1, and the downregulated gene IL17RB) consistent with the previously reported role of oxaliplatin during immune cell death [55]. These analyses also highlighted several genes involved in cell architecture, namely cytoskeleton and junctional complexes. Amongst the most striking features were changes in the expression of integrin and extracellular matrix proteins engaging Integrins and Focal Adhesions: collagens COL5A1 and COL12A1, as well as laminins LAMA3, LAMB3, and LAMC1 and integrin ITGA3. These observations suggest that treated cells might remodel their extracellular matrix, their Focal Adhesions, and the signaling pathways associated. The RNA-Seq analyses also revealed many changes to the cytoskeleton, including an upregulation of several keratin-based intermediate filaments (KRT15/19/32) and associated factors (KRTAP2-3 and SFN). Several genes controlling the actin cytoskeleton were also affected such as the branched actin regulators WDR63, CYFIP2, or WASF3, or different genes predicted to control RHO activity (up: RHOD, EZR, and RAP2; down: ARHGAP18).

Importantly, when considering the role of the Hippo pathway during resistance in CRC, with the exception of AXL, none of the "classic" YAP/TAZ target genes such as CTGF, CYR61/CCN1, or BIRC2 were up-regulated after oxaliplatin treatment. Similarly, none of the reported YAP/TAZ target genes involved in cell cycle progression, cytoskeleton regulation, or drug resistance [41, 57] were up-regulated in response to oxaliplatin. This suggests that either YAP/TAZ-mediated transcription is not activated following oxaliplatin, or that it controls an alternative YAP/TAZ program, specific to the oxaliplatin and/or DNA damage cellular context. Indeed, performing pathway analyses on the mis-regulated genes did not highlight any signature for Hippo signaling. However, it highlighted a strong activation of p53 signaling (Supplemental Table S2), and motif enrichment analyses suggested that the p53 family of transcription factors were the main controllers of the up-regulated genes.

Taken together, these results suggest that upon oxaliplatin treatment, HCT116 cells implement an early cell death program, which is likely mediated by the elevated p53 levels, and many "bona-fide" p53 direct target genes involved in cell death are upregulated. Unlike other treatments such as cisplatin, doxorubicin, and etoposide [26, 52], oxaliplatin is unlikely to mobilize the p73 antitumoral response since p73 levels are decreased upon oxaliplatin treatment. The difference is striking when considering closely related platinum compounds such as cisplatin and oxaliplatin. This difference is unlikely due to timing as we could not observe any p73 up-regulation after oxaliplatin treatment even after shorter or longer exposures. Even though dose comparisons between different compounds is tricky, we note that the cisplatin dose was 50 times higher than that of oxaliplatin. Alternatively, while both are thought to act primarily as generators of lethal amounts of DNA breaks, their difference in mobilizing either p73 (cisplatin) or p53 (oxaliplatin) might arise from different alternative cellular effects independent of DNA damage.

YAP or TAZ are dispensable for Oxaliplatin-mediated cell death

Our results on the role of the Hippo pathway during sensitivity to oxaliplatin treatment suggests therefore that although the Hippo pathway appears downregulated, and that TAZ accumulates in the nucleus of treated cells at 24 h, this does not lead to the activation of previously reported YAP/TAZ target genes [41, 57]. We thus wondered what would be the role of YAP and TAZ in the response to oxaliplatin treatment. Indeed, other anti-cancer drugs such as cisplatin have been shown to promote cell death in part through the implementation of a p73/YAP-dependent cell death program. Mechanistically, it has been proposed that DNA damage induced by cisplatin stabilizes YAP which then binds and protects p73 from ITCH-mediated degradation [28]; the p73/YAP complex accumulates in the nucleus to turn on the expression of p73 target genes involved in cell death [26, 52, 53]. We thus wondered whether the accumulation of TAZ (and the moderate accumulation

of YAP) in the nucleus could also participate in the cell death induced by oxaliplatin.

To test the requirement of YAP and TAZ, we invalidated YAP and TAZ by RNA interference. The sole invalidation of YAP by shRNA or TAZ by siRNA led to a very modest reduction in oxaliplatin sensitivity (IC50 in *shYAP* or siTAZ were determined at 0.62 and 0.59 respectively compared to 0.52 in *shLuc* controls) (Fig. 3A&C). It is noteworthy that, under the culture conditions used, YAP appeared dispensable for HCT116 cells since the shRNA led to a knock-down efficiency > 90%. We could not formerly assess whether normal TAZ levels were required for cell survival as we used siRNA whose action is limited in time. The fact that YAP depletion alone does not increase the IC50 suggests that the cell death in response to oxaliplatin might not be dependent (or only marginally) on the YAP/p73 complex as previously reported for other DNA-damage inducing compounds [26, 28, 52], but depends on alternative mechanisms.

YAP and TAZ sensitize to cell death in response to oxaliplatin

We then investigated whether YAP and TAZ could act redundantly. Strikingly, while the depletion of YAP or TAZ had hardly any effect, the combined knock-down of both YAP (*shYAP*) and TAZ (*siTAZ*), resulted in a clear increase in resistance to oxaliplatin, where the IC50 reached 0.91 µM in *shYAP/siTAZ* HCT116 cells compared to 0.58 µM in *shLuc/siScrambled* HCT116 control cells (Fig. 3B&C), highlighting that YAP and TAZ participate to cell death in response to oxaliplatin. The effects observed were specific to the *siTAZ*, since we observed a re-sensitization of treated cells when complementing them with an expression vector for a murine version of *Taz* insensitive to the *siTAZ* designed against human *TAZ* (Fig. 3D&E). We then wondered whether the increased sensitivity promoted by TAZ could be dependent on p73, in a similar mechanism as proposed for cisplatin. However, while p53 accumulated in response to oxaliplatin in HCT116, p73 levels were decreased, undermining the role of p73 in response to this drug (Fig. 1C). This absence of p73 stabilization is consistent with the absence of increased YAP levels after oxaliplatin treatment (Fig. 2B). These results highlight that, although overexpressed YAP could bind and stabilize endogenous p73 (Supplemental Figure S3A; [28, 52, 53]), oxaliplatin treatments at the clinically relevant doses used, do not lead to YAP and p73 stabilization. We then confirmed that TAZ cannot bind p73 (Supplemental Figure S3A), ruling out that the elevated nuclear TAZ following oxaliplatin could act through a transcriptional complex with p73 to enhance cell death. A recent study reported a direct interaction between TAZ and p53 in MCF7 and HCT116 cells, which resulted in the inhibition of p53 activity towards senescence [35]. However, when we performed co-immunoprecipitation experiments, we were unable to document any interaction between over-expressed YAP or overexpressed TAZ with endogenous p53 in normal or oxaliplatin treated HCT116 cells (Supplemental Figure S3A). Furthermore, the increased oxaliplatin resistance of cells upon *YAP/TAZ* knockdown supports strongly that YAP and TAZ act to promote cell death and thus cooperate with p53 rather than antagonize its activity as suggested before [35]. Taken together, these results suggest that the sensitivity of HCT116 cells to oxaliplatin mediated by YAP and TAZ is not mediated by the direct interaction of YAP or TAZ to p53 or p73.

Increased resistance to oxaliplatin upon YAP/TAZ activity blockade

The sh/siRNA interference results suggested that YAP and TAZ were required for sensitivity to oxaliplatin. To validate independently the knock-down experiments,

(See figure on next page.)

Fig. 3 YAP and TAZ accelerate oxaliplatin-mediated cell death. **A** HCT116-*shLuc*, HCT116-*shYAP*, and HCT116 transfected with *siTAZ* were treated with increasing doses of oxaliplatin for 96 h. Cell viability analysis was then assessed using SRB assay and the IC50 of oxaliplatin was calculated as the concentration needed to kill 50% of the cells (shown in the inset). One-way ANOVA statistical test, * $p < 0.05$. **B** HCT116-*shYAP-siTAZ* and HCT116-*shLuc-siCtl* (control) cell lines were treated with increasing doses of oxaliplatin for 96 h. Cell viability analysis was then assessed using SRB assay and the IC50 of oxaliplatin was calculated as the concentration needed to kill 50% of the cells (shown in the inset). Paired two-tailed Student's t-test, ** $p < 0.01$. **C** Western blot analysis showing protein expression of TAZ and YAP in HCT116-*shLuc*, *-siTAZ*, *-shYAP* and both *-shYAP-siTAZ* used in panel A and B. Tubulin was used as a loading control ($n = 3$). **D** HCT116-*shYAP-siScramb* (control), HCT116-*shYAP-siTAZ*, and HCT116-*shYAP-siTAZ* transfected with a Flag tagged murine Taz *(pEFmTaz)* cell lines were treated with increasing doses of oxaliplatin for 96 h. Cell viability analysis was then assessed using SRB assay and the IC50 of oxaliplatin was calculated as the concentration needed to kill 50% of the cells. Paired two-tailed Student's t-test, ** $p < 0.01$, ns non-significant. **E** Western blot analysis showing protein expression of TAZ and Flag in the different cell lines used in panel D. GAPDH was used as a loading control. **F** HCT116 cells were incubated with increasing concentrations of oxaliplatin and either Verteporfin or CA3. Cell viability was assessed with the SRB assay in 2D to obtain the viability matrix. Drug concentrations were as follows: Verteporfin (from 0.437 to 7 µM), CA3 (from 0.004 to 0.75 µM) and Oxaliplatin (from 0.0185 to 1.2 µM). The synergy matrices were calculated as described in "Materials and methods" section

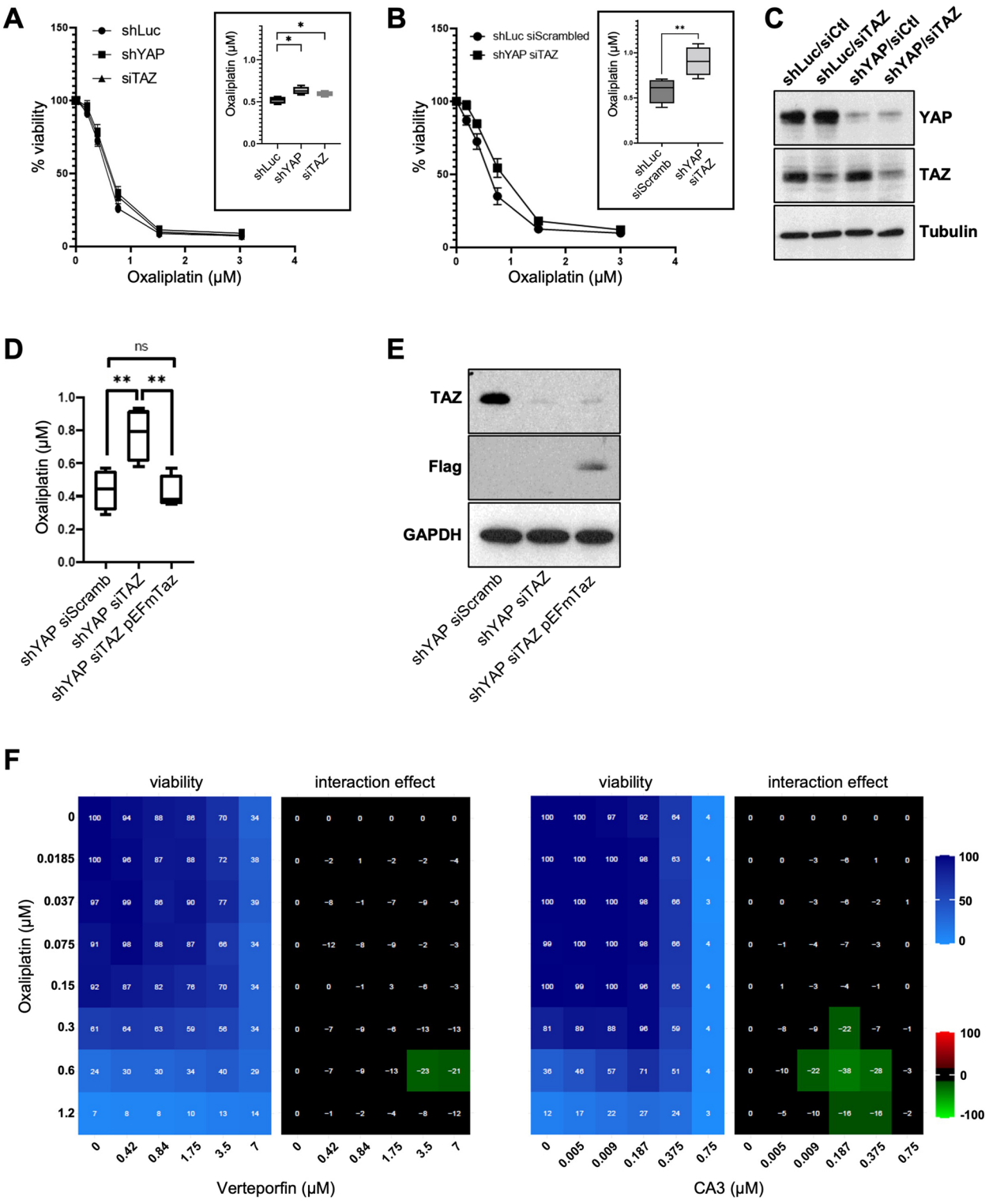

Fig. 3 (See legend on previous page.)

we used a pharmacological approach with drugs targeting YAP/TAZ activity and monitored their action in combination with oxaliplatin. We performed 2D matrices co-treatment analyses in which cells were treated with increasing amounts of oxaliplatin and of the YAP/TAZ inhibitors verteporfin or CA3 (Fig. 3G

and Supplemental Figure S1B &C; [34, 50]). In both cases, the co-treatments led to a marked increase in the HCT116 resistance to oxaliplatin. The mode of action of verteporfin remains unclear and might involve increased retention in the cytoplasm of YAP and TAZ, or their degradation, preventing them from complexing in the nucleus with their transcription factor partners [60]. A recent study showed that CA3 reduced the transcriptional activity mediated by YAP/TAZ-TEAD (reduction in target genes expression), with only minor effects on YAP protein levels [36]. Even though the exact mode of action of verteporfin and CA3 remain unclear, the increased resistance to oxaliplatin observed by co-treating cells with YAP/TAZ pharmacological inhibitors, confirms the results obtained with the genetic knock-down. Given that the effects of oxaliplatin on protein accumulation and nuclear relocalization were mostly seen for TAZ, our results support a model where increased TAZ activity participate in the sensitivity of CRC cells to oxaliplatin.

The p53 status of cancer cells impacts the role of YAP/TAZ on oxaliplatin sensitivity

We then tested different CRC cell lines to test whether the antagonism between YAP/TAZ inhibition and oxaliplatin treatment is specific to HCT116 cells. Transcriptomic analysis of treated HCT116 cells highlighted a major p53 signature (Supplemental Tables S1 and 2), suggesting that cell death and sensitivity to oxaliplatin might be strongly influenced by the p53 status of the cells. We obtained similar results as for HCT116 with the p53 wild-type LoVo cells (nuclear TAZ relocalization and antagonism with Verteporfin and CA3; Fig. 4A&B). The importance of a wild-type p53 context was further supported by the observation that HCT116 cells mutant for p53 (deletion of the first exon; [7]) completely abolished the antagonism between YAP/TAZ drugs and oxaliplatin (Fig. 5A).

We then investigated different CRC cell lines mutant for p53: HT-29 (mutation R273H), SW480 (mutation R273H), and Caco-2 (mutation E204*). We did not observe any interaction between anti YAP/TAZ drugs and oxaliplatin in HT-29 and SW480 cells, consistent with the importance of the p53 context (Fig. 5B&C). However, in Caco-2 cells, the fourth p53 mutant cell line tested, we could observe an antagonism between oxaliplatin and verteporfin or CA3 treatments, similar to what was observed for the p53 wild-type HCT116 and LoVo cells (Fig. 5D). Amongst the p53 mutant CRC cells, Caco-2 appear thus to behave differently. The reason remains to be identified, but this might be dependent on the type of p53 mutation. Indeed, it is now well established that the different p53 mutations are not equivalent and confer specific behaviors [10]. Another reason might be the epithelial characteristics of Caco-2 cells. Indeed, unlike most other CRC cell lines, Caco-2 retain highly organized intercellular junctions, and can form epithelial sheets [37].

Together these results suggest that the antagonism between anti YAP/TAZ drug and oxaliplatin might be dependent on a wild-type p53 status. The situation in p53 mutants cells appears more diverse with most cell lines tested showing independent actions of the drugs.

Src inhibition by Dasatinib reduces HCT116 cells sensitivity to oxaliplatin

The results suggest thus that preventing TAZ signaling in the early phases of oxaliplatin treatment would represent a counter-productive approach, leading to reduced efficacy of oxaliplatin to induce cell death. Besides the canonical Hippo signaling pathway, the nucleo-cytoplasmic shuttling of YAP and TAZ is under the control of many other inputs. In particular, YAP and TAZ retention in the nucleus is promoted by the action of different tyrosine kinases, such as ABL or SFKs (Src Family Kinases) which phosphorylate the C-termini of YAP and TAZ (Y357 or Y316 respectively; [8, 13, 16, 21, 25, 30]). Due to its high relevance for colon cancer, we focused our analysis on SRC, frequently activated in colon carcinoma [49]. An earlier study showed that depending on the colon cancer cell line considered, SRC could be activated, inhibited, or not affected following oxaliplatin treatment [24]. We could replicate that SRC was not activated after 24 h of oxaliplatin treatment in HCT116 cells (as measured by phosphorylation on Y416; Fig. 6A). Working with HCT116, we are thus in a position to test the contribution of SRC to YAP/TAZ shuttling during oxaliplatin treatment without the complications arising from treatment-induced acute SRC activation. Previous reports suggested that the classic SRC kinase inhibitor Dasatinib could be used as a drug to prevent YAP/TAZ signaling [46]. Indeed, combining Dasatinib with oxaliplatin treatment, prevented the nuclear accumulation of TAZ (Fig. 6B). The addition of Dasatinib to oxaliplatin treated cells led to a dramatic reduction of the TAZ nuclear staining when compared to oxaliplatin alone (95% reduction; see "Materials and methods" section. It should be noted however, that Dasatinib treatment at 50 nM reduced slightly the elevated global TAZ levels observed in response to oxaliplatin (Fig. 6A). Nevertheless, even though TAZ appeared a bit more unstable in presence of Dasatinib, its nucleo-cytoplasmic ratio

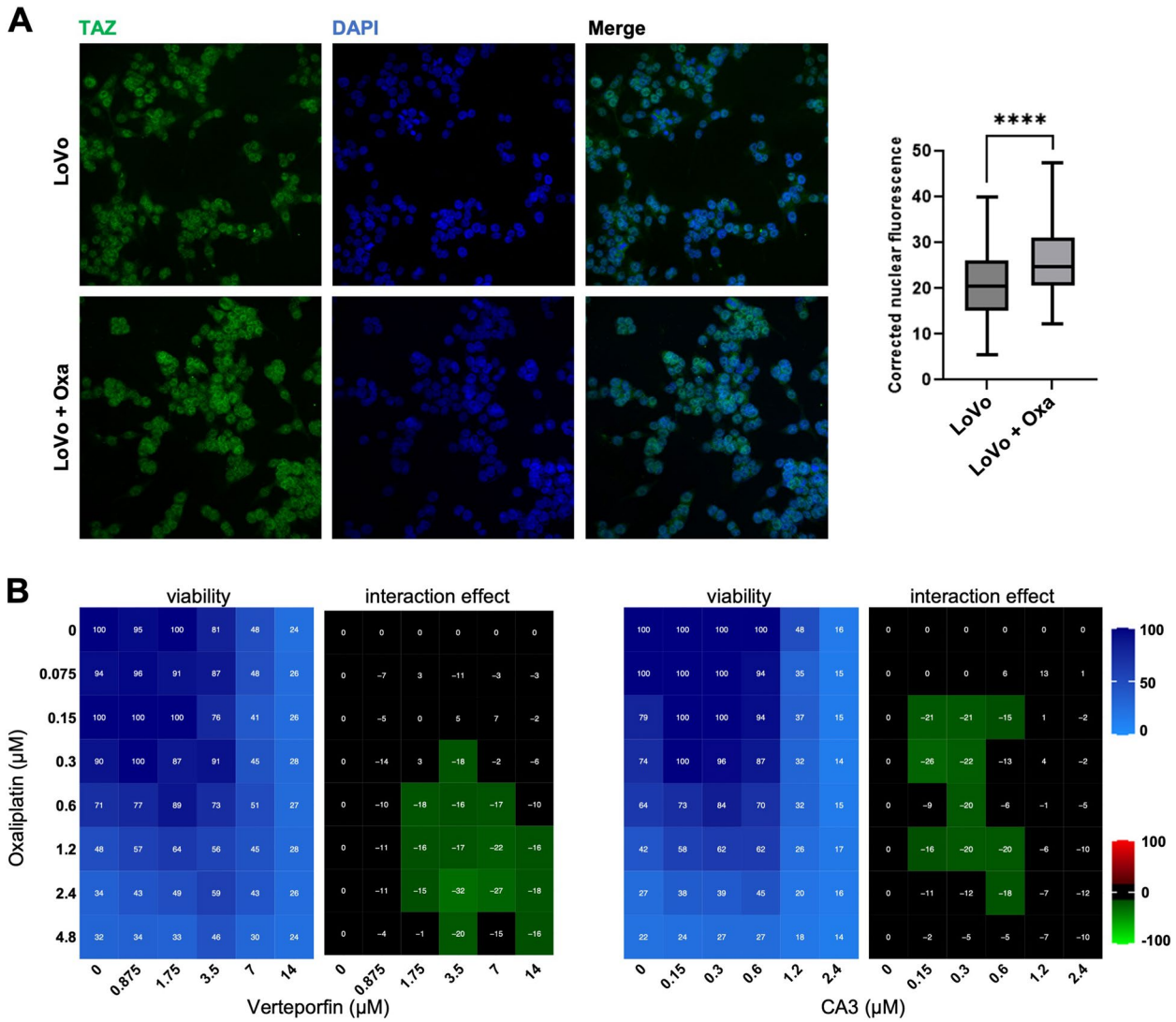

Fig. 4 Oxaliplatin treatment effects in LoVo cells. **A** Immunofluorescence experiments performed on LoVo cells treated or not, with oxaliplatin at IC50 (0.6 μM) monitoring TAZ nuclear localization (green). DAPI (blue) was used to stain DNA and the nuclei. Quantifications are shown on the right side of the figure and are represented as the corrected nuclear fluorescence. Data are represented as the mean ± SEM. Unpaired two-tailed Student's t-test; **** $p < 0.0001$. **B** LoVo cells were incubated with increasing concentrations of oxaliplatin and either Verteporfin or CA3. Cell viability was assessed with the SRB assay in 2D to obtain the viability matrix. Drug concentrations were as follows: Verteporfin (from 0.875 to 14 μM), CA3 (from 0.15 to 2.4 μM) and Oxaliplatin (from 0.075 to 4.8 μM). The synergy matrices were calculated as described in "Materials and methods" section

was still profoundly affected by Dasatinib, preventing nuclear accumulation (Fig. 6B).

We thus asked what would be the combined effect of Dasatinib treatment and oxaliplatin in HCT116 cells. We thus performed 2D matrices co-treatment analyses in which cells were treated with increasing amounts of oxaliplatin and of Dasatinib using drug ranges encompassing their respective IC50 (0.5 μM for oxaliplatin and 8 μM for Dasatinib; Supplemental Figure S1A&D). Strikingly combining both drugs showed clear regions of antagonism, suggesting that Dasatinib treatment reduced HCT116 cells sensitivity to oxaliplatin (Fig. 6C). These results further support a model in which the nuclear relocalization of TAZ in response to oxaliplatin treatment sensitizes cells, and caution the use of Dasatinib in combination to oxaliplatin.

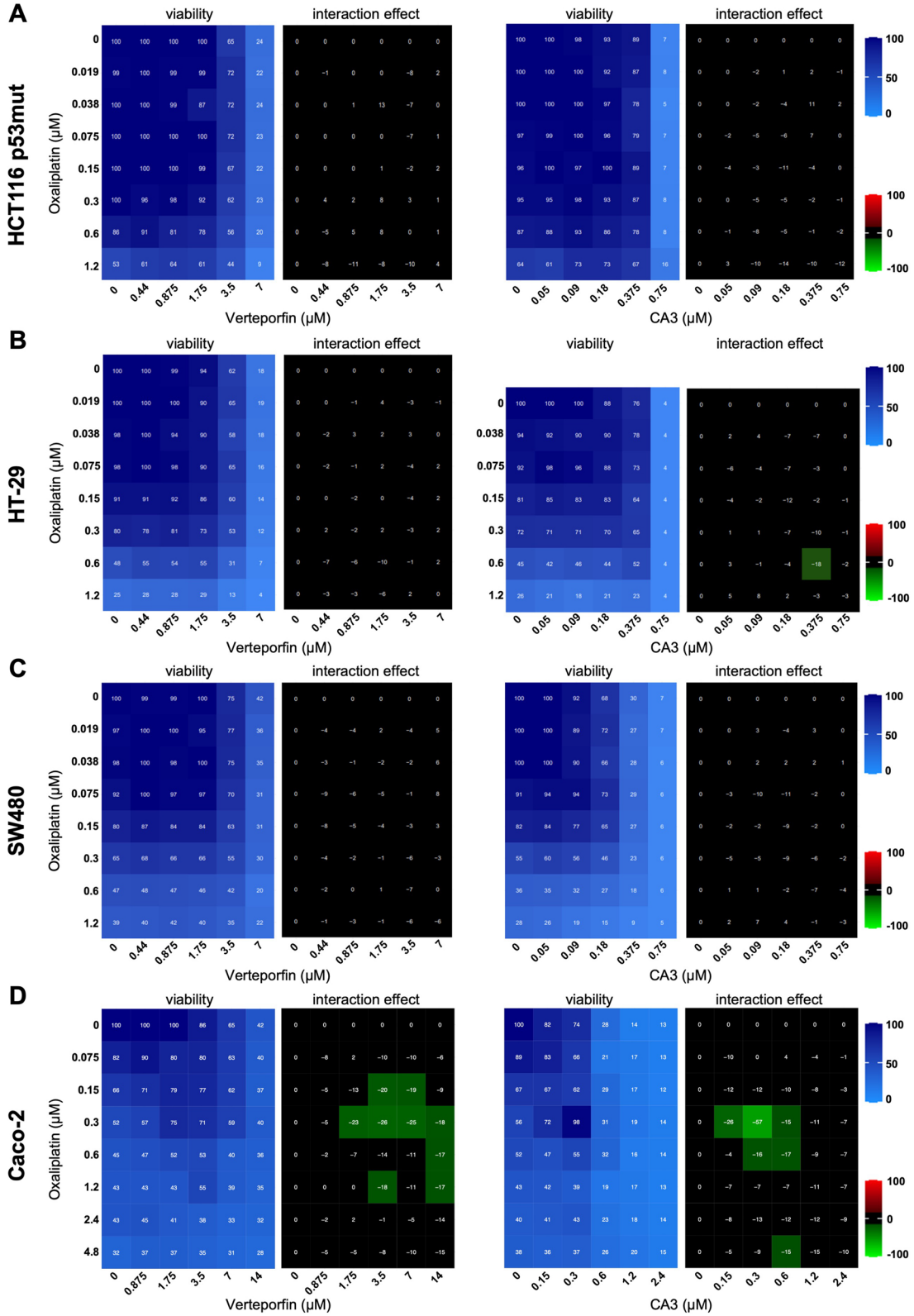

Fig. 5 Oxaliplatin and YAP/TAZ drugs interactions in p53 mutant CRC cell lines. **A-D** HCT116 p53mut (**A**), HT-29 (**B**), SW480 (**C**), and Caco-2 (**D**) cells were incubated with increasing concentrations of oxaliplatin and either Verteporfin or CA3. Cell viability was assessed with the SRB assay in 2D to obtain the viability matrix. The synergy matrices were calculated as described in "Materials and methods" section

YAP/TAZ promote cell death in the early response to chemotherapeutic agents

Taken together the results presented here show that oxaliplatin promotes the fast nuclear relocalization of TAZ which then participates to the cells sensitivity to oxaliplatin. Given that we could not find any interaction between TAZ and p53 family members, but that the nuclear localization of TAZ is required for its effect, we could envision several models:

i) either the TAZ/TEAD transcription complex, in the context of DNA damage and p53 activation, promotes the transcription of specific early response genes promoting cell death;
ii) or the slight increase at the transcriptional level of "classic" YAP/TAZ/TEAD targets involved in proliferation sensitizes cells to DNA damage and replicative stress (*shYAP/siTAZ* HCT116 cells proliferated less rapidly than control cells which might protect them from the damages induced by oxaliplatin; Supplemental Figure S3B);
iii) or alternatively, TAZ acts through a new complex involved in cell death, independently of TEAD.

More studies should help to distinguish between these potential models.

YAP and TAZ, have been implicated in the resistance to various chemotherapies or targeted therapies in different cancers [22, 38, 65]. It should be noted that the current study focuses on the immediate effects of oxaliplatin within the first hours after exposure. Whether YAP and TAZ are later important for the maintenance of the resistance acquired by the surviving clones is not addressed in this study. Hints towards this later role of YAP/TAZ, are suggested by the elevated YAP levels reported in many cancer cells following resistant clone selection (our own unpublished results, and [22, 38, 65]. Functional studies impairing YAP demonstrated that YAP is indeed required for the tumorigenicity of resistant cells [64]. Furthermore, elevated YAP and TAZ nuclear staining is frequently observed in patients tumor samples, including in CRCs [29, 33, 51, 56]. In advanced cancers, almost all patients undergo one or more rounds of treatment before surgery, if surgery is possible. It is thus unclear whether the increased YAP/TAZ nuclear levels observed in tumor samples reflect primary response to treatment (as suggested by the current study), or whether they represent a secondary state that might have been selected in the cells resistant to treatment.

The Hippo core kinases MST1/2 and LATS1/2 represent the main regulators of YAP and TAZ activities. These core Hippo pathway kinases have also been implicated in CRC [11, 31]. But it should be noted that YAP/TAZ stability and nuclear localization are also regulated by alternative mechanisms independent of the Hippo core kinases, such as mechanical cues, cytoplasmic trapping by AMOTs [17, 41, 66] or by their C-terminal phosphorylation on key tyrosine residues [8, 13, 30]. Thus, although oxaliplatin treated cells showed signs of lower Hippo core kinase activity, the current study did not formerly establish whether core Hippo kinases were involved in the sensitivity of CRC cells to oxaliplatin.

The current study investigates the early response to oxaliplatin, supporting an early tumor suppressive role of YAP/TAZ in response to treatment, in which, in the context of detrimental DNA damage and a wild type p53 activity, YAP/TAZ activity promotes cell death. Is this role general or is it specific to CRCs and oxaliplatin? Independently of the mechanism involved (YAP/p73 complex as previously reported or alternative TAZ-mediated mechanisms as shown here), different breast and colon cancer cell lines mobilize YAP or TAZ to promote cell death in response to many different DNA damaging agents [6, 26, 28, 52, 53]. This anti-tumoral role appears evolutionarily conserved and in *Drosophila* the YAP/TAZ homologue Yki promotes cell death in response to different stress inducing agents [12], further suggesting that YAP/TAZ might promote cell

(See figure on next page.)

Fig. 6 Src inhibition by Dasatinib reduces HCT116 cells sensitivity to oxaliplatin. **A** Western blot analysis showing protein expression of YAP and TAZ in HCT116 treated, or not, with oxaliplatin (0.5 µM) and/or Dasatinib (50 nM and 100 nM). Phopsho-SRC blotting was used to evaluate the inhibition of SRC activity using Dasatinib. GAPDH was used as a loading control ($n=3$). Quantification of the blots (performed using Image J software) is shown on the right side of the figure. **B** Immunofluorescence experiments performed in HCT116 cells treated, or not, with oxaliplatin (0.5 µM) and/or Dasatinib (50 nM) monitoring YAP (top panels) and TAZ (bottom panels) nuclear localization (red). DAPI (blue) was used to stain DNA and the nuclei. Quantification of both stainings are shown on the right side of the figures and are represented as the corrected nuclear fluorescence. Data are represented as the mean ± SEM ($n=3$). Unpaired two-tailed Student's t-test; ****$p<0.0001$. **C** HCT116 colorectal cancer cell lines were incubated with increasing concentrations of oxaliplatin and Dasatinib. Cell viability was assessed with the SRB assay in 2D to obtain the viability matrix. Drug concentrations were as follows: Dasatinib (from 1 to 16 µM) and oxaliplatin (from 0.0185 to 1.2 µM). The synergy matrix was calculated as described in "Materials and methods" section

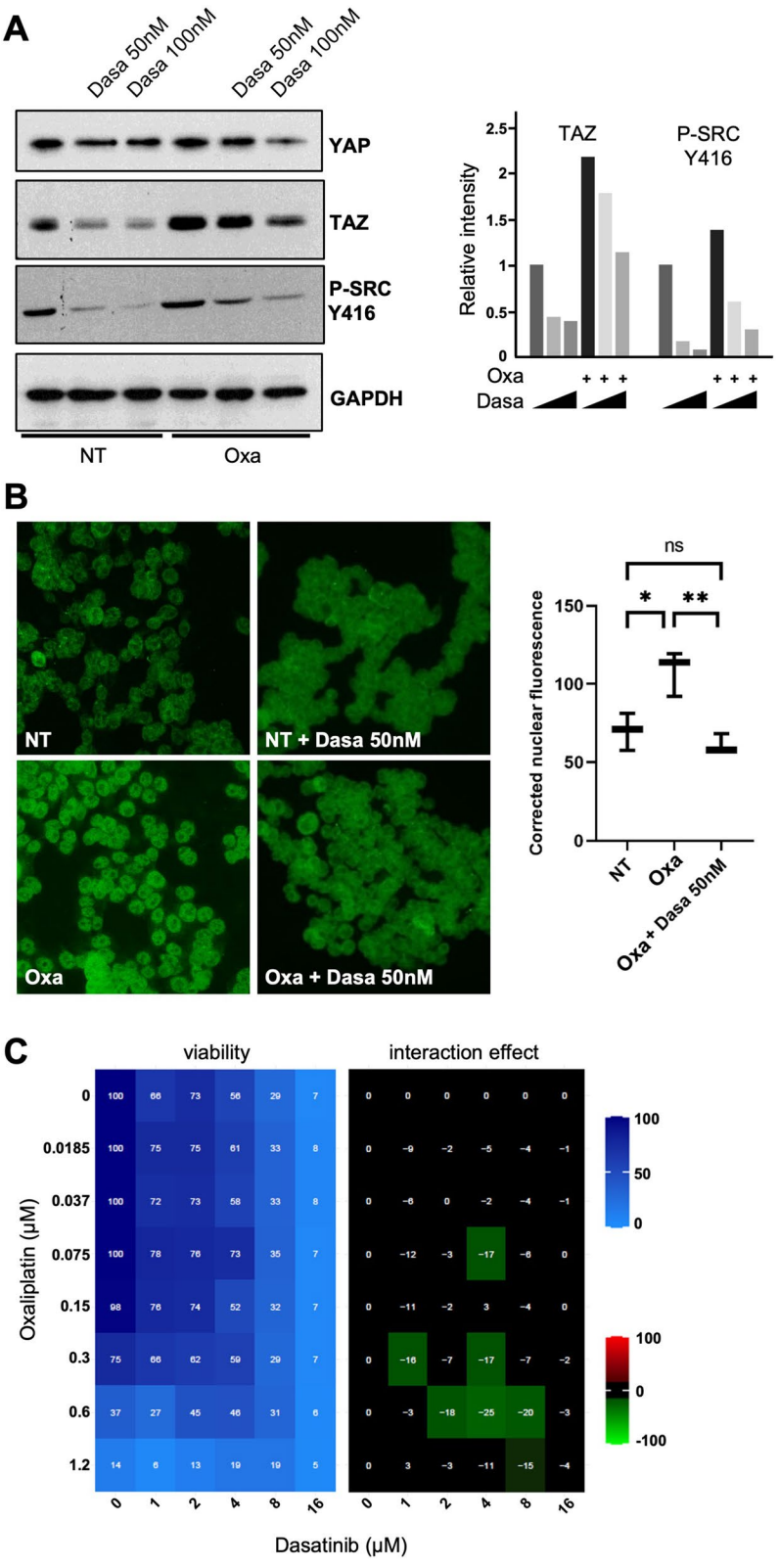

Fig. 6 (See legend on previous page.)

death in response to chemotherapeutic agents in other cancers beside CRCs and breast cancers. When considering drugging YAP/TAZ signaling in the treatment of CRCs and other cancers, special attention should thus be given to drug combinations, and importantly the sequence in which they will be used, in particular for tumors with wild-type p53.

Abbreviations

53BP1	53 Binding Protein-1
5-FU	5-Fluorouracil
AMOT	Angiomotin
BSA	Bovine serum albumin
CRC	Colorectal cancer
CTCF	Corrected total cell fluorescence
CTGF	Connective tissue growth factor
EGFR	Epidermal growth factor receptor
IC50	Half maximal inhibitory concentration
LATS	Large tumor suppressor
MOB1	Mps one binder kinase activator 1
MSI	Microsatellite instable
MST	Mammalian Ste20-like
NF2	Neurofibromatosis type 2
ns	Not significant
NT	Not treated
Oxa	Oxaliplatin
PBS	Phosphate buffer saline
RIN	RNA integrity number
SEM	Standard error of the mean
SFK	Src family kinase
shRNA	Short hairpin RNA
siRNA	Small interfering RNA
SRB	Sulforhodamine B
TAZ	Transcriptional coactivator with PDZ-binding motif
TEAD	TEA domain transcription factor (TEA = TEF-1 and AbaA)
TF	Transcription factor
VEGF	Vascular endothelial growth factor
WWTR1	WW domain containing transcription regulator 1
YAP	Yes associated protein
Yki	Yorkie

Supplementary Information

The online version contains supplementary material available at https://doi.org/10.1186/s12885-024-12316-4.

Supplementary Material 1.

Supplementary Material 2.

Supplementary Material 3.

Acknowledgements
The authors thank the different lab members of the Djiane and Gongora teams for helpful discussions.

Authors' contributions
Conceptualization: AD. Formal analysis: VS, LHM, MR, AD. Funding acquisition: AD, CG, VS, LHM. Investigation: VS, LHM, LJ, DK. Methodology: CG, DT. Project administration: AD. Resources: CG, LB. Software: DT, CG, LB. Supervision: AD, CG. Validation: DK, LJ, AA. Visualization: VS, LHM, MR, AD. Writing—original draft: AD, CG. Writing—review & editing: AD, CG, VS, LHM.The work reported in the paper has been performed by the authors, unless clearly specified in the text.

Funding
VS was supported by Fondation de France. MR was supported by LabEx NUMEV. DK was supported by Ligue Nationale Contre le Cancer. This work was supported by grants from Fondation ARC (#PJA 20141201630) and Ligue Nationale Contre le Cancer (Région Languedoc-Roussillon) to LHM and AD. Work in the lab of CG was also supported by grants and funds from INSERM, the Institut du cancer de Montpellier (ICM), SIRIC (SIRIC Montpellier Cancer Grant «INCa-DGOS-Inserm 6045»), Cancéropole GSO, and the program «investissement d'avenir» (grant agreement: Labex MabImprove, ANR-10-LABX-53-01).

Availability of data and materials
The raw RNA-Seq data generated in this study is available in GEO under accession number GSE227315. Other data that support the findings of this study are available from the corresponding authors upon request.

Declarations

Ethics approval and consent to participate
Not applicable.

Consent for publication
Not applicable.

Competing interests
The authors declare no competing interests.

Received: 25 September 2023 Accepted: 29 April 2024
Published online: 14 May 2024

References

1. Abuetabh Y, Wu HH, Chai C, Al Yousef H, Persad S, Sergi CM, Leng R. DNA damage response revisited: the p53 family and its regulators provide endless cancer therapy opportunities. Exp Mol Med. 2022;54:1658–69. https://doi.org/10.1038/s12276-022-00863-4.
2. Anders S, Huber W. Differential expression analysis for sequence count data. Genome Biol. 2010;11:R106. https://doi.org/10.1186/gb-2010-11-10-r106.
3. Azzolin L, Panciera T, Soligo S, Enzo E, Bicciato S, Dupont S, Bresolin S, Frasson C, Basso G, Guzzardo V, Fassina A, Cordenonsi M, Piccolo S. YAP/TAZ incorporation in the β-catenin destruction complex orchestrates the Wnt response. Cell. 2014;158:157–70. https://doi.org/10.1016/j.cell.2014.06.013.
4. Azzolin L, Zanconato F, Bresolin S, Forcato M, Basso G, Bicciato S, Cordenonsi M, Piccolo S. Role of TAZ as mediator of Wnt signaling. Cell. 2012;151:1443–56. https://doi.org/10.1016/j.cell.2012.11.027.
5. Barry ER, Morikawa T, Butler BL, Shrestha K, de la Rosa R, Yan KS, Fuchs CS, Magness ST, Smits R, Ogino S, Kuo CJ, Camargo FD. Restriction of intestinal stem cell expansion and the regenerative response by YAP. Nature. 2013;493:106–10. https://doi.org/10.1038/nature11693.
6. Basu S, Totty NF, Irwin MS, Sudol M, Downward J. Akt phosphorylates the Yes-associated protein, YAP, to induce interaction with 14–3-3 and attenuation of p73-mediated apoptosis. Mol Cell. 2003;11:11–23. https://doi.org/10.1016/s1097-2765(02)00776-1.
7. Bunz F, Dutriaux A, Lengauer C, Waldman T, Zhou S, Brown JP, Sedivy JM, Kinzler KW, Vogelstein B. Requirement for p53 and p21 to sustain G2 arrest after DNA damage. Science. 1998;282:1497–501. https://doi.org/10.1126/science.282.5393.1497.
8. Byun MR, Hwang J-H, Kim AR, Kim KM, Park JI, Oh HT, Hwang ES, Hong J-H. SRC activates TAZ for intestinal tumorigenesis and regeneration. Cancer Lett. 2017;410:32–40. https://doi.org/10.1016/j.canlet.2017.09.003.
9. Chaney S. The chemistry and biology of platinum complexes with the 1,2-diaminocyclohexane carrier ligand (review). Int J Oncol. 1995;6:1291–305. https://doi.org/10.3892/ijo.6.6.1291.
10. Chen X, Zhang T, Su W, Dou Z, Zhao D, Jin X, Lei H, Wang J, Xie X, Cheng B, Li Q, Zhang H, Di C. Mutant p53 in cancer: from molecular mechanism to therapeutic modulation. Cell Death Dis. 2022;13:974. https://doi.org/10.1038/s41419-022-05408-1.
11. Cheung P, Xiol J, Dill MT, Yuan W-C, Panero R, Roper J, Osorio FG, Maglic D, Li Q, Gurung B, Calogero RA, Yilmaz ÖH, Mao J, Camargo FD. Regenerative

reprogramming of the intestinal stem cell state via Hippo signaling suppresses metastatic colorectal cancer. Cell Stem Cell. 2020;27:590-604.e9. https://doi.org/10.1016/j.stem.2020.07.003.
12. Di Cara F, Maile TM, Parsons BD, Magico A, Basu S, Tapon N, King-Jones K. The Hippo pathway promotes cell survival in response to chemical stress. Cell Death Differ. 2015;22:1526–39. https://doi.org/10.1038/cdd.2015.10.
13. Ege N, Dowbaj AM, Jiang M, Howell M, Hooper S, Foster C, Jenkins RP, Sahai E. Quantitative analysis reveals that actin and Src-family kinases regulate nuclear YAP1 and its export. Cell Syst. 2018;6:692-708.e13. https://doi.org/10.1016/j.cels.2018.05.006.
14. Graham MA, Lockwood GF, Greenslade D, Brienza S, Bayssas M, Gamelin E. Clinical pharmacokinetics of oxaliplatin: a critical review. Clin Cancer Res. 2000;6:1205–18.
15. Greco WR, Bravo G, Parsons JC. The search for synergy: a critical review from a response surface perspective. Pharmacol Rev. 1995;47:331–85.
16. Guégan J-P, Lapouge M, Voisin L, Saba-El-Leil MK, Tanguay P-L, Lévesque K, Brégeon J, Mes-Masson A-M, Lamarre D, Haibe-Kains B, Trinh VQ, Soucy G, Bilodeau M, Meloche S. Signaling by the tyrosine kinase Yes promotes liver cancer development. Sci Signal. 2022;15:eabj4743. https://doi.org/10.1126/scisignal.abj4743.
17. Heng BC, Zhang X, Aubel D, Bai Y, Li X, Wei Y, Fussenegger M, Deng X. An overview of signaling pathways regulating YAP/TAZ activity. Cell Mol Life Sci. 2021;78:497–512. https://doi.org/10.1007/s00018-020-03579-8.
18. Ho KC, Zhou Z, She Y-M, Chun A, Cyr TD, Yang X. Itch E3 ubiquitin ligase regulates large tumor suppressor 1 stability [corrected]. Proc Natl Acad Sci U S A. 2011;108:4870–5. https://doi.org/10.1073/pnas.1101273108.
19. Kanai F, Marignani PA, Sarbassova D, Yagi R, Hall RA, Donowitz M, Hisaminato A, Fujiwara T, Ito Y, Cantley LC, Yaffe MB. TAZ: a novel transcriptional co-activator regulated by interactions with 14–3-3 and PDZ domain proteins. EMBO J. 2000;19:6778–91. https://doi.org/10.1093/emboj/19.24.6778.
20. Kantar D, Mur EB, Mancini M, Slaninova V, Salah YB, Costa L, Forest E, Lassus P, Géminard C, Boissière-Michot F, Orsetti B, Theillet C, Colinge J, Benistant C, Maraver A, Heron-Milhavet L, Djiane A. MAGI1 inhibits the AMOTL2/p38 stress pathway and prevents luminal breast tumorigenesis. Sci Rep. 2021;11:5752. https://doi.org/10.1038/s41598-021-85056-1.
21. Kedan A, Verma N, Saroha A, Shreberk-Shaked M, Müller A-K, Nair NU, Lev S. PYK2 negatively regulates the Hippo pathway in TNBC by stabilizing TAZ protein. Cell Death Dis. 2018;9:985. https://doi.org/10.1038/s41419-018-1005-z.
22. Kim MH, Kim J. Role of YAP/TAZ transcriptional regulators in resistance to anti-cancer therapies. Cell Mol Life Sci. 2017;74:1457–74. https://doi.org/10.1007/s00018-016-2412-x.
23. Konsavage WM, Kyler SL, Rennoll SA, Jin G, Yochum GS. Wnt/β-catenin signaling regulates Yes-associated protein (YAP) gene expression in colorectal carcinoma cells. J Biol Chem. 2012;287:11730–9. https://doi.org/10.1074/jbc.M111.327767.
24. Kopetz S, Lesslie DP, Dallas NA, Park SI, Johnson M, Parikh NU, Kim MP, Abbruzzese JL, Ellis LM, Chandra J, Gallick GE. Synergistic activity of the SRC family kinase inhibitor dasatinib and oxaliplatin in colon carcinoma cells is mediated by oxidative stress. Cancer Res. 2009;69:3842–9. https://doi.org/10.1158/0008-5472.CAN-08-2246.
25. Lamar JM, Xiao Y, Norton E, Jiang Z-G, Gerhard GM, Kooner S, Warren JSA, Hynes RO. SRC tyrosine kinase activates the YAP/TAZ axis and thereby drives tumor growth and metastasis. J Biol Chem. 2019;294:2302–17. https://doi.org/10.1074/jbc.RA118.004364.
26. Lapi E, Di Agostino S, Donzelli S, Gal H, Domany E, Rechavi G, Pandolfi PP, Givol D, Strano S, Lu X, Blandino G. PML, YAP, and p73 are components of a proapoptotic autoregulatory feedback loop. Mol Cell. 2008;32:803–14. https://doi.org/10.1016/j.molcel.2008.11.019.
27. Lee K-W, Lee SS, Kim S-B, Sohn BH, Lee H-S, Jang H-J, Park Y-Y, Kopetz S, Kim SS, Oh SC, Lee J-S. Significant association of oncogene YAP1 with poor prognosis and cetuximab resistance in colorectal cancer patients. Clin Cancer Res. 2015;21:357–64. https://doi.org/10.1158/1078-0432.CCR-14-1374.
28. Levy D, Adamovich Y, Reuven N, Shaul Y. The Yes-associated protein 1 stabilizes p73 by preventing Itch-mediated ubiquitination of p73. Cell Death Differ. 2007;14:743–51. https://doi.org/10.1038/sj.cdd.4402063.
29. Li F-L, Guan K-L. The two sides of Hippo pathway in cancer. Semin Cancer Biol. 2022;85:33–42. https://doi.org/10.1016/j.semcancer.2021.07.006.
30. Li P, Silvis MR, Honaker Y, Lien W-H, Arron ST, Vasioukhin V. αE-catenin inhibits a Src-YAP1 oncogenic module that couples tyrosine kinases and the effector of Hippo signaling pathway. Genes Dev. 2016;30:798–811. https://doi.org/10.1101/gad.274951.115.
31. Li Q, Sun Y, Jarugumilli GK, Liu S, Dang K, Cotton JL, Xiol J, Chan PY, DeRan M, Ma L, Li R, Zhu LJ, Li JH, Leiter AB, Ip YT, Camargo FD, Luo X, Johnson RL, Wu X, Mao J. Lats1/2 sustain intestinal stem cells and Wnt activation through TEAD-dependent and independent transcription. Cell Stem Cell. 2020;26:675-692.e8. https://doi.org/10.1016/j.stem.2020.03.002.
32. Lignitto L, Arcella A, Sepe M, Rinaldi L, Delle Donne R, Gallo A, Stefan E, Bachmann VA, Oliva MA, Tiziana Storlazzi C, L'Abbate A, Brunetti A, Gargiulo S, Gramanzini M, Insabato L, Garbi C, Gottesman ME, Feliciello A. Proteolysis of MOB1 by the ubiquitin ligase praja2 attenuates Hippo signalling and supports glioblastoma growth. Nat Commun. 2013;4:1822. https://doi.org/10.1038/ncomms2791.
33. Ling H-H, Kuo C-C, Lin B-X, Huang Y-H, Lin C-W. Elevation of YAP promotes the epithelial-mesenchymal transition and tumor aggressiveness in colorectal cancer. Exp Cell Res. 2017;350:218–25. https://doi.org/10.1016/j.yexcr.2016.11.024.
34. Liu-Chittenden Y, Huang B, Shim JS, Chen Q, Lee S-J, Anders RA, Liu JO, Pan D. Genetic and pharmacological disruption of the TEAD-YAP complex suppresses the oncogenic activity of YAP. Genes Dev. 2012;26:1300–5. https://doi.org/10.1101/gad.192856.112.
35. Miyajima C, Kawarada Y, Inoue Y, Suzuki C, Mitamura K, Morishita D, Ohoka N, Imamura T, Hayashi H. Transcriptional coactivator TAZ negatively regulates tumor suppressor p53 activity and cellular senescence. Cells. 2020;9:171. https://doi.org/10.3390/cells9010171.
36. Morice S, Mullard M, Brion R, Dupuy M, Renault S, Tesfaye R, Brounais-Le Royer B, Ory B, Redini F, Verrecchia F. The YAP/TEAD axis as a new therapeutic target in osteosarcoma: effect of verteporfin and CA3 on primary tumor growth. Cancers (Basel). 2020;12:3847. https://doi.org/10.3390/cancers12123847.
37. Natoli M, Leoni BD, D'Agnano I, D'Onofrio M, Brandi R, Arisi I, Zucco F, Felsani A. Cell growing density affects the structural and functional properties of Caco-2 differentiated monolayer. J Cell Physiol. 2011;226:1531–43. https://doi.org/10.1002/jcp.22487.
38. Nguyen CDK, Yi C. YAP/TAZ signaling and resistance to cancer therapy. Trends Cancer. 2019;5:283–96. https://doi.org/10.1016/j.trecan.2019.02.010.
39. Panatta E, Zampieri C, Melino G, Amelio I. Understanding p53 tumour suppressor network. Biol Direct. 2021;16:14. https://doi.org/10.1186/s13062-021-00298-3.
40. Perego P, Robert J. Oxaliplatin in the era of personalized medicine: from mechanistic studies to clinical efficacy. Cancer Chemother Pharmacol. 2016;77:5–18. https://doi.org/10.1007/s00280-015-2901-x.
41 Pocaterra A, Romani P, Dupont S. YAP/TAZ functions and their regulation at a glance. J Cell Sci. 2020;133:jcs230425. https://doi.org/10.1242/jcs.230425.
42. Raudvere U, Kolberg L, Kuzmin I, Arak T, Adler P, Peterson H, Vilo J. g:Profiler: a web server for functional enrichment analysis and conversions of gene lists (2019 update). Nucleic Acids Res. 2019;47:W191–8. https://doi.org/10.1093/nar/gkz369.
43. Rawla P, Sunkara T, Barsouk A. Epidemiology of colorectal cancer: incidence, mortality, survival, and risk factors. Prz Gastroenterol. 2019;14:89–103. https://doi.org/10.5114/pg.2018.81072.
44. Raymond E, Faivre S, Woynarowski JM, Chaney SG. Oxaliplatin: mechanism of action and antineoplastic activity. Semin Oncol. 1998;25:4–12.
45. Reggiani F, Gobbi G, Ciarrocchi A, Sancisi V. YAP and TAZ are not identical twins. Trends Biochem Sci. 2021;46:154–68. https://doi.org/10.1016/j.tibs.2020.08.012.
46. Rosenbluh J, Nijhawan D, Cox AG, Li X, Neal JT, Schafer EJ, Zack TI, Wang X, Tsherniak A, Schinzel AC, Shao DD, Schumacher SE, Weir BA, Vazquez F, Cowley GS, Root DE, Mesirov JP, Beroukhim R, Kuo CJ, Goessling W, Hahn WC. β-Catenin-driven cancers require a YAP1 transcriptional complex for survival and tumorigenesis. Cell. 2012;151:1457–73. https://doi.org/10.1016/j.cell.2012.11.026.
47. Salah Z, Melino G, Aqeilan RI. Negative regulation of the Hippo pathway by E3 ubiquitin ligase ITCH is sufficient to promote tumorigenicity. Cancer Res. 2011;71:2010–20. https://doi.org/10.1158/0008-5472.CAN-10-3516.
48. Shao DD, Xue W, Krall EB, Bhutkar A, Piccioni F, Wang X, Schinzel AC, Sood S, Rosenbluh J, Kim JW, Zwang Y, Roberts TM, Root DE, Jacks T, Hahn WC. KRAS and YAP1 converge to regulate EMT and tumor survival. Cell. 2014;158:171–84. https://doi.org/10.1016/j.cell.2014.06.004.
49. Sirvent A, Mevizou R, Naim D, Lafitte M, Roche S. Src family tyrosine kinases in intestinal homeostasis, regeneration and tumorigenesis. Cancers (Basel). 2020;12:E2014. https://doi.org/10.3390/cancers12082014.

50. Song S, Xie M, Scott AW, Jin J, Ma L, Dong X, Skinner HD, Johnson RL, Ding S, Ajani JA. A novel YAP1 inhibitor targets CSC-enriched radiation-resistant cells and exerts strong antitumor activity in esophageal adenocarcinoma. Mol Cancer Ther. 2018;17:443–54. https://doi.org/10.1158/1535-7163.MCT-17-0560.
51. Steinhardt AA, Gayyed MF, Klein AP, Dong J, Maitra A, Pan D, Montgomery EA, Anders RA. Expression of Yes-associated protein in common solid tumors. Hum Pathol. 2008;39:1582–9. https://doi.org/10.1016/j.humpath.2008.04.012.
52. Strano S, Monti O, Pediconi N, Baccarini A, Fontemaggi G, Lapi E, Mantovani F, Damalas A, Citro G, Sacchi A, Del Sal G, Levrero M, Blandino G. The transcriptional coactivator Yes-associated protein drives p73 gene-target specificity in response to DNA Damage. Mol Cell. 2005;18:447–59. https://doi.org/10.1016/j.molcel.2005.04.008.
53. Strano S, Munarriz E, Rossi M, Castagnoli L, Shaul Y, Sacchi A, Oren M, Sudol M, Cesareni G, Blandino G. Physical interaction with Yes-associated protein enhances p73 transcriptional activity. J Biol Chem. 2001;276:15164–73. https://doi.org/10.1074/jbc.M010484200.
54. Tapon N, Harvey KF, Bell DW, Wahrer DCR, Schiripo TA, Haber DA, Hariharan IK. salvador promotes both cell cycle exit and apoptosis in Drosophila and is mutated in human cancer cell lines. Cell. 2002;110:467–78. https://doi.org/10.1016/s0092-8674(02)00824-3.
55. Tesniere A, Schlemmer F, Boige V, Kepp O, Martins I, Ghiringhelli F, Aymeric L, Michaud M, Apetoh L, Barault L, Mendiboure J, Pignon J-P, Jooste V, van Endert P, Ducreux M, Zitvogel L, Piard F, Kroemer G. Immunogenic death of colon cancer cells treated with oxaliplatin. Oncogene. 2010;29:482–91. https://doi.org/10.1038/onc.2009.356.
56. Thompson BJ. YAP/TAZ: drivers of tumor growth, metastasis, and resistance to therapy. BioEssays. 2020;42:e1900162. https://doi.org/10.1002/bies.201900162.
57. Totaro A, Panciera T, Piccolo S. YAP/TAZ upstream signals and downstream responses. Nat Cell Biol. 2018;20:888–99. https://doi.org/10.1038/s41556-018-0142-z.
58. Touil Y, Igoudjil W, Corvaisier M, Dessein A-F, Vandomme J, Monté D, Stechly L, Skrypek N, Langlois C, Grard G, Millet G, Leteurtre E, Dumont P, Truant S, Pruvot F-R, Hebbar M, Fan F, Ellis LM, Formstecher P, Van Seuningen I, Gespach C, Polakowska R, Huet G. Colon cancer cells escape 5FU chemotherapy-induced cell death by entering stemness and quiescence associated with the c-Yes/YAP axis. Clin Cancer Res. 2014;20:837–46. https://doi.org/10.1158/1078-0432.CCR-13-1854.
59. Vasan N, Baselga J, Hyman DM. A view on drug resistance in cancer. Nature. 2019;575:299–309. https://doi.org/10.1038/s41586-019-1730-1.
60. Wang C, Zhu X, Feng W, Yu Y, Jeong K, Guo W, Lu Y, Mills GB. Verteporfin inhibits YAP function through up-regulating 14-3-3σ sequestering YAP in the cytoplasm. Am J Cancer Res. 2016;6:27–37.
61. Woynarowski JM, Chapman WG, Napier C, Herzig MC, Juniewicz P. Sequence- and region-specificity of oxaliplatin adducts in naked and cellular DNA. Mol Pharmacol. 1998;54:770–7. https://doi.org/10.1124/mol.54.5.770.
62. Woynarowski JM, Faivre S, Herzig MC, Arnett B, Chapman WG, Trevino AV, Raymond E, Chaney SG, Vaisman A, Varchenko M, Juniewicz PE. Oxaliplatin-induced damage of cellular DNA. Mol Pharmacol. 2000;58:920–7. https://doi.org/10.1124/mol.58.5.920.
63. Xie Y-H, Chen Y-X, Fang J-Y. Comprehensive review of targeted therapy for colorectal cancer. Signal Transduct Target Ther. 2020;5:22. https://doi.org/10.1038/s41392-020-0116-z.
64. Yoshikawa K, Noguchi K, Nakano Y, Yamamura M, Takaoka K, Hashimoto-Tamaoki T, Kishimoto H. The Hippo pathway transcriptional co-activator, YAP, confers resistance to cisplatin in human oral squamous cell carcinoma. Int J Oncol. 2015;46:2364–70. https://doi.org/10.3892/ijo.2015.2948.
65. Zeng R, Dong J. The Hippo signaling pathway in drug resistance in cancer. Cancers (Basel). 2021;13:318. https://doi.org/10.3390/cancers13020318.
66. Zheng Y, Pan D. The Hippo signaling pathway in development and disease. Dev Cell. 2019;50:264–82. https://doi.org/10.1016/j.devcel.2019.06.003.

Publisher's Note